

Trade Science Inc.

# Materials Science

*An Indian Journal***Full Paper**

MSAIJ, 5(4), 2009 [334-341]

## Corrosion inhibition and adsorption behavior of new 2,3bis-((2-aminoethoxy)dimethylsilyloxy)-N-(2-(2-aminoethylamino)ethyl)-4,5,6-trihydroxyhex-2-enamide (AEDSHE) on carbon steel surfaces in 0.5 M hydrochloric acid

O.M.Abo-Elenien<sup>1,\*</sup>, K.M.Zohdy<sup>2</sup>, M.Abd-Elkreem<sup>2</sup>, Olfat.E.Elazabawy<sup>1</sup><sup>1</sup>Egyptian Petroleum Research Institute (EPRI), Nasr city 11727, Cairo, (EGYPT)<sup>2</sup>Higher Technological Institute, 10 th of Ramadan City, (EGYPT)

E-mail : drossamaa12@yahoo.com

Received: 22<sup>nd</sup> June, 2009 ; Accepted: 2<sup>nd</sup> July, 2009

### ABSTRACT

2,3bis-((2-aminoethoxy)dimethylsilyloxy)-N-(2-(2-aminoethylamino)ethyl)-4,5,6-trihydroxyhex-2-enamide (AEDSHE) has been synthesized and evaluated as a corrosion inhibitor. The inhibitive action of inhibitor AEDSHE at concentration 0.0, 5.0, 10.0, 20.0, 30.0, and 40.0 ppm on the corrosion of Carbon Steel in 0.5MHCl solutions was evaluated by open circuit potential, potentiodynamic polarization, electrochemical impedance spectroscopy and weight loss measurements. All the studied showed good inhibitive characteristics against the corrosion of Carbon Steel. Polarization data indicated that the studied compound is cathodic inhibitor without changing the mechanism of hydrogen evolution reaction. The adsorption of inhibitor on Carbon Steel obeys Langmuir adsorption isotherm. The morphology of the formed films was also examined by scanning electron microscope (SEM) and EDX.

© 2009 Trade Science Inc. - INDIA

### KEYWORDS

Carbon steel;  
Inhibitor and  
electrochemical polarization.

### INTRODUCTION

Petroleum fields are the biggest victim of corrosion and severe economic loss is caused due to the metallic corrosion on piping and plant stems. Statistical data show that failures by corrosion in the oil and gas industry oscillate between 25% and 30% of the total losses<sup>[1-3]</sup>. Different methods are used for protection of corrosion in petroleum product pipeline and plants in aggressive environments, where one of the most economic methods is the application of corrosion inhibitors (CIs)<sup>[4-10]</sup>.

The use of organic inhibitors in acid solutions is very

common way in protection of metals, particularly in view of the high corrosion rate<sup>[11-17]</sup>. Amines, ammonium salts and organoamide compounds are well known corrosion inhibitors for iron and its alloys. Their relatively high water solubility is an advantage for use as corrosion inhibitors<sup>[8-19]</sup>.

Most of the effective organic inhibitors used contain heteroatom such as O, N, S and multiple bonds in their molecules through which they are adsorbed on the metal surface<sup>[20-26]</sup>. It has been observed that adsorption depends mainly on certain physico-chemical properties of the inhibitor group, such as electron density at

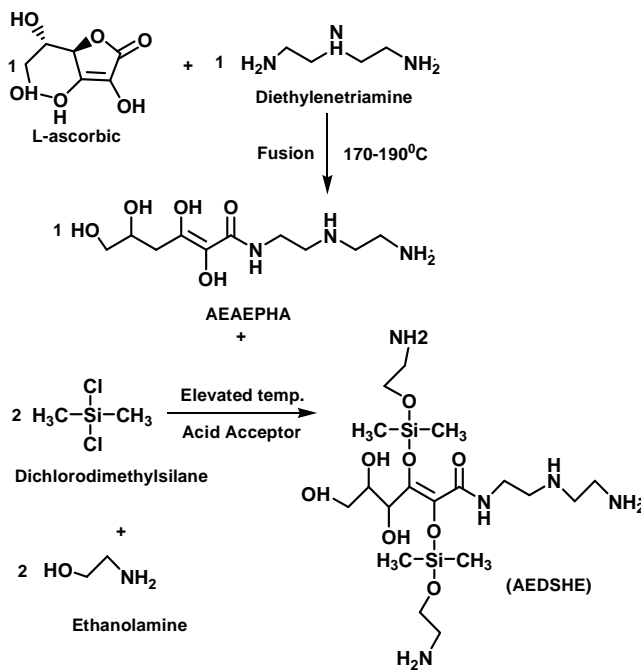
the donor atom,  $\pi$ -orbital character, and the electronic structure of the molecule<sup>[27]</sup>. In general, an increase in temperature, in the case of physical adsorption, reduces corrosion rate by increasing the inhibitor efficiency due to its adsorption on the metal surface. Thus, finding an inhibitor with high efficiency at low and high temperature is of substantial economic significance<sup>[25-27]</sup>.

In this work, synthesis of AEDSHE and was studied as corrosion inhibitor. The influence of inhibitor concentration on the corrosion rate, efficiency and inhibition mechanism in aqueous 0.5M HCl solution on carbon steel as the working electrode were investigated by using weight loss, electrochemical polarization and surface morphology by scanning electron microscope (SEM) and EDX.

## MATERIALS AND METHODS

### Procedure for the synthesis of AEDSHE

In free solvent three neck flask 1.0 M of L-ascorbic acid and 1.0 M of Diethylenetriamine heated at 160°C for 3 hrs and cooling at 25 °C, then added 2.0 M of Dichlorodimethylsilane and 2.0 M of Ethanolamine in presence of acid acceptor and heated at evaluated temperature. The product is purified and confirmed by FT.IR.



### Infra-red Spectral characterization of inhibitor (AEDSHE)

The product obtained were characterized by using Infra red (FT.IR) resonance spectroscopy. PerkinElmer, Paragon 500 model Mattson – infinity series bench top 961. The spectrum was taken in the mid-IR region of 400–4000cm<sup>-1</sup>.

## CORROSION STUDY

### Surface preparation of carbon steel

The carbon steel alloy type 410 containing, 0.12% Ti, 0.085 % V, 11.27% Cr, 0.557% Mn, 0.354% Co, 0.077% Cu, 0.027% Zn, 0.009% Mo and the remainder Fe were used in this study. The test specimens were used in the form of sheets (2×2×0.2) cm, and of 6g average weight, the specimens were first mechanically polished with emery paper from 240 to 1200 grit to obtain a smooth surface degreased with acetone, then washed with double distilled water, and finally dried between two filter papers and weighed

### Weight loss measurements

For the weight loss method the specimens were cleaned and dried. The weight of each specimen was measured before and after immersion in 0.5 M HCl for 12 h in the absence and presence of different concentrations of corrosion inhibitor 0.0, 5.0, 10.0, 20.0, 30.0 and 40.0 ppm. The change in weight was recorded to the nearest 0.0001g. A blank experiment was carried out simultaneously using M HCL solution without inhibitor. The weight loss was given by

$$\Delta W = W_1 - W_2 \quad (1)$$

Where  $W_1$  and  $W_2$  are the weight of specimen before and after immersion, respectively. The inhibition efficiency % I was computed by the equation:

$$I\% = \frac{\Delta W - \Delta W_i}{\Delta W} \times 100 \quad (2)$$

Where  $\Delta W$  and  $\Delta W_i$  are the weight losses per unit area in absence and presence of the inhibitors, respectively. The corrosion rate was then calculated as:

$$mpy = \frac{KW}{DAT} \quad (3)$$

Where,  $K = 3.45 \times 10^6$ ,  $W$  = weight loss.  $D$  = density of specimen in g cm<sup>-3</sup>,  $A$  = area of specimen, (cm<sup>2</sup>) and  $T$  = exposure time, (hours).

## Full Paper

The coverage surface area

$$\theta = \frac{\Delta W - \Delta W_i}{\Delta W} \quad (4)$$

### Electrochemical measurements

Electrochemical experiments were carried out in a glass cell (CEC/TH-Radiometer) with a capacity of 100 ml. A platinum electrode and saturated calomel electrode (SCE) were used as a counter electrode and a reference electrode. The working electrode (WE) was in the form of a disc cut from c. steel under investigation and was embedded in a Teflon rod with an exposed area of 0.867 cm<sup>2</sup>. Electrochemical impedance spectroscopy (EIS), potentiodynamic and linear polarization were conducted in an electrochemical measurement system (VoltaLab40) which comprises a PGZ301 potentiostat, a personal computer and VoltaMaster 4 and Zview software.

The potentiodynamic current-potential curves were recorded by changing the electrode potential automatically from -800 to 0 mV with scanning rate of 5 mV s<sup>-1</sup>. The polarization resistance measurements were performed by applying a controlled potential scan over a small range typically 15 mV with respect to Ecorr. The resulting current is linearly plotted versus potential, the slope of this plot at Ecorr being the polarization resistance (Rp). All experiments were carried out in freshly prepared solution at room temperatures. The ac impedance measurements were performed at corrosion potentials (Ecorr) over a frequency range of 100 kHz-10 mHz, with a signal amplitude perturbation of 10 mV. Nyquist plots were obtained.

### Scanning electron microscopy (SEM) and (EDX) microscopy

A JEOL (5300 Japan) scanning electron microscope were utilized to examine the surface morphology of various specimens of carbon steel alloy in case of polished surface only and those immersed in 0.5 M hydrochloric acid in absence and presence of inhibitor at 30.0 ppm for 24 hr. This instrument was operated in a secondary electron imaging mode with an accelerating voltage of either 10 or 20 KeV. In the present investigation two magnifications were selected, 750 and 2000X.

## RESULTS AND DISCUSSION

### FTIR spectroscopy analyses

Figure 1 shows that the characteristic diagram for AEDSHE compound. The band appeared at 519 cm<sup>-1</sup> for stretching vibration of the aliphatic straight chain – C–C– skeleton, the band appeared at 749 cm<sup>-1</sup> for stretching vibration of –(CH<sub>2</sub>)<sub>2</sub>– groups, the band appeared at 1078 cm<sup>-1</sup> for stretching vibration of the primary –CH<sub>2</sub>–OH group, the bands appeared at 1135 and 1340 cm<sup>-1</sup> for stretching vibration of –CH(OH)– groups, the band appeared at 1627 cm<sup>-1</sup> for stretching vibration of the –C=C– group conjugated with –C=O group, the bands appeared at 2303, 2381 and 3424 cm<sup>-1</sup> for stretching vibration of –NH– and –NH<sub>2</sub> groups and the band appeared at 2959 cm<sup>-1</sup> for stretching vibration of the –CONH– group. The band appeared at 598 cm<sup>-1</sup> for stretching vibration of the primary –CH<sub>2</sub>–OH group, the band appeared at 801 cm<sup>-1</sup> for stretching vibration of CH<sub>3</sub>–Si–CH<sub>3</sub> group, the band appeared at 914 cm<sup>-1</sup> for stretching vibration of CH<sub>2</sub>–NH–CH<sub>2</sub> group, the band appeared at 1025 cm<sup>-1</sup> for stretching vibration of the primary –NH<sub>2</sub> group, the bands appeared at 1078, 1258 and 1401 cm<sup>-1</sup> for stretching vibration of –CH(OH)– groups.

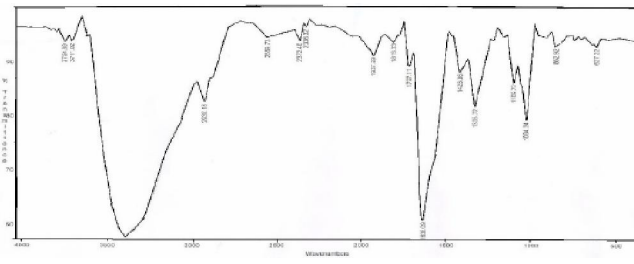
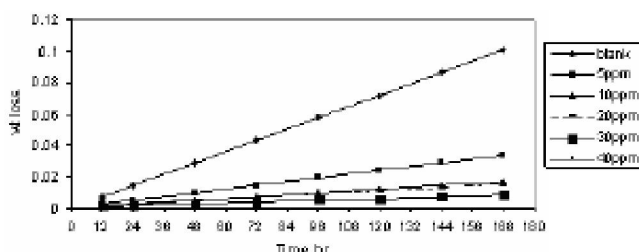


Figure 1 : I.R spectra of (AEDSHE) inhibitor

### Weight loss method

The weight loss of carbon steel specimens immersed in 0.5M HCl solution decreased with increasing concentration of AEDSHE (Figure 2). This indicates that this compound has a retardation effect on the dissolution of steel by the action of the acid. In the other words, it acts as a corrosion inhibitor, probably through the formation of barrier film between the metal surface and the acidic medium. The linear variation of weight loss versus time of immersion suggests the absence of insoluble surface films during the corrosion process.



**Figure 2 : Weight loss- time curves form carbon steel in 0.5M HCl in absence and presence of different concentrations of the inhibitor**

The mechanism of inhibitor may occur by adsorption of the inhibitor on the metal surface and then impedance of corrosion is affected either by merely blocking the reaction sites or by altering the mechanism of the anodic and cathodic partial processes. The formation of films on the surface of the metal appears to be due to chemisorptions of active, amino amide, siloxane and hydroxyl groups through nitrogen, silicon and oxygen atoms which can donate their unshared electron pairs to Fe leading to protective film. Furthermore, the rate of corrosion ( $K$ ) decreases with increasing the inhibitor concentration (TABLE 1 & Figure 3).

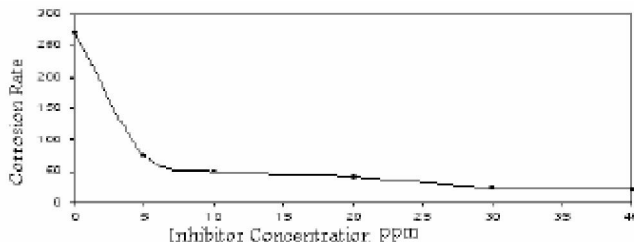


**Figure 3 : Effect of concentration of the inhibitor on the corrosion rate of carbon steel in 0.5M HCl after 168hrs**

**TABLE 1 : Corrosion inhibition of the inhibitor at different concentrations in 0.5MHCl, at 298 K**

Concentration (ppm)	Rate of corrosion (mpy)	Coverage surface ( $\theta$ )	Efficiency (I%)
blank	271	-	-
5	75	0.7232	72.32
10	51	0.8128	81.28
20	42	0.8465	84.65
30	25	0.9096	90.96
40	22	0.9181	91.81

It is not worthy that the efficiency of inhibition increases with increasing the concentration of the tested

compound, (TABLE 1, Figure 4), which probably suggests the formation multilayer of molecules on the surface of the metal causing a shielding for the metal from coming in contact with the acid solution. This effect also agrees with calculation of the coverage area ( $\theta$ ) which shows a direct relation with the concentration of the compound under examination.

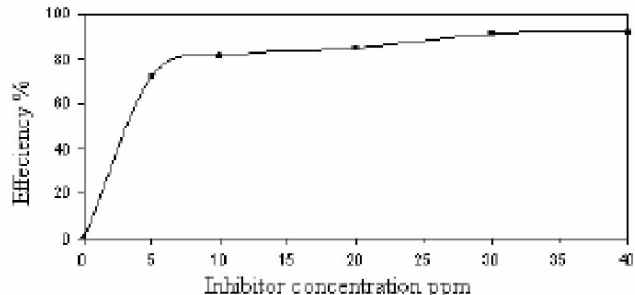


**Figure 4 : Effect of concentration of the inhibitor on the efficiency of carbon steel in 0.5M HCl after 168 hr**

**Adsorption isotherm:** The data obtained for  $\theta$  summarized in TABLE 1. Shows that, there is an inverse relation between the rate of corrosion and the surface coverage area. The  $\theta$  value near unity indicates almost a full coverage of the metal surface and consequently  $\theta$  is considered as a good barrier shielding the corroding surface from corrosive medium and retarding the corrosion rate of carbon steel.

From Langmuir plots (Figure 5), it is found that, the investigated compound show linear plots which suggests that it obeys Langmuir adsorption represented by the following equation:

$$\log C = \log \theta / 1 - \theta - \log A \quad (5)$$

$$\log A = -1.74 - \Delta G / 2.303RT \quad (6)$$

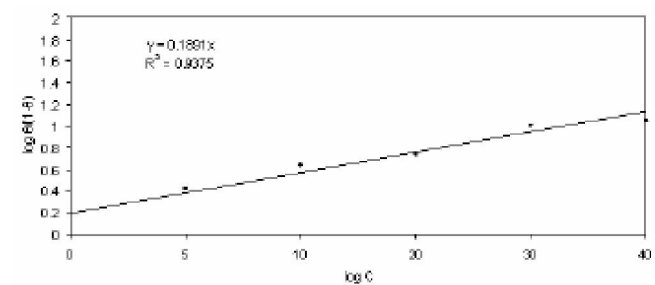


**Figure 5 : Dependence of Log  $\theta$  / 1 -  $\theta$  concentration for the inhibitor**

The slope of this isotherm deviates from unity which assumes that, there is no interaction between the

## Full Paper

adsorbed molecules, however in practice; there is a mutual repulsion or attraction between the adsorbed species on the metal surface<sup>[12]</sup>.

### The effect of temperature with respect to activation and thermodynamic parameters

Comparison of Figure 6 and Figure 7, shows that addition of 40 ppm of AEDSHE greatly suppressed the dissolution of steel in 0.5 M HCl although in absence or presence of this compound corrosion increases with raising the temperature of the aid solution, yet the weight loss was much less in the presence of the addition, which means that the compound is effective in both low and relatively high temperature (35 – 65 °C). The values of corrosion rate obtained at different temperatures permit the calculation of the Arrhenius activation energy,  $E_a^*$ , according to the following equation

$$\log K = -E_a^*/2.303RT + \log A \quad (7)$$

Where A is the Arrhenius pre-exponential factor, a constant which depends on the metal type and the electrolyte, K is the corrosion rate, R is the universal gas constant and T is the absolute temperature.

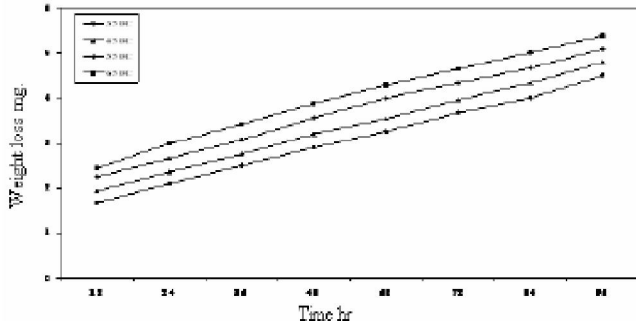


**Figure 6 : Weight loss- time curve of carbon steel in 0.5M HCl at different temperature**

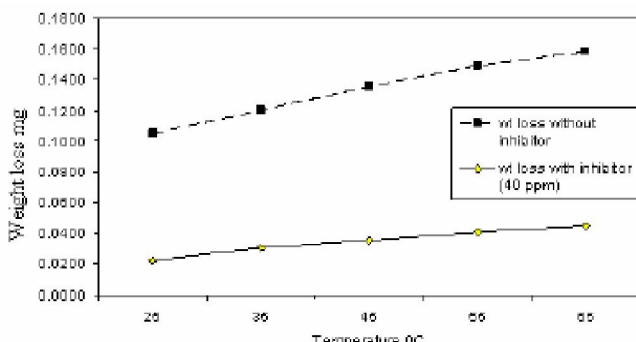


**Figure 7 : Weight loss- time curve of carbon steel in 0.5M HCl in presence 40ppm of inhibitor at different temperature**

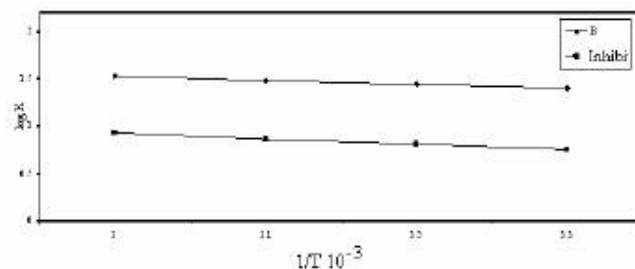


**Figure 8 : Log K and 1/T curve for C steel dissolution in 0.5M HCl in presence of 40ppm of inhibitor at different temperature**

**TABLE 2 : The following is the thermodynamic parameters at different temperatures**

T	$\Delta G$	$\Delta H$	$\Delta S$
298	9.458	-517.99	-1.7
308	9.775	-434.858	-1.44
318	10.093	-351.718	-1.1377
328	10.41	-268.578	-0.85
338	10.728	-185.438	-0.58

### Open circuit potential measurements (OCP).

Figure 9 illustrates the variation of the potential of carbon steel electrode as a function of the period of exposure was measured against (SCE). It is clear that, the corrosion potential of carbon steel electrode in 0.5M HCl solution (blank curve) tends towards more negative value firstly, giving rise to short step, which represents the break down of the pre-immersion, air formed oxide film present on the surface according to the equation:



This is followed by the growth of a new oxide film inside the solution, so that the potential was shifted again to more noble direction until steady state potential is established. Additions of the inhibitor molecules produce a positive shift in  $E_{corr}$  and as the concentration

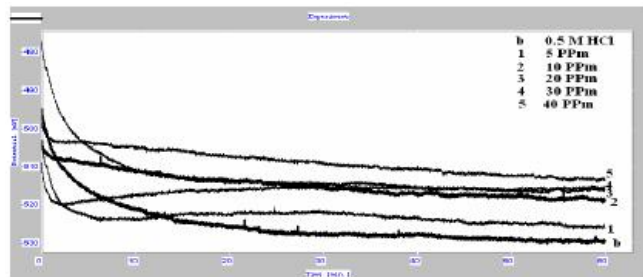


**Figure 9 : Potential-time curves for mild steel in 0.5M HCl in absence and presence of various concentrations of the inhibitor**

of the inhibitor increases; the corrosion potential was shifted to more noble direction

### Electrochemical polarization measurements

Potentiodynamic polarization curves (Figure 10) for carbon steel alloy in 0.5M HCl solution and in presence of 5, 10, 20 30 AND 40 ppm of the AEDSHE compound as well as some electrochemical parameters, namely, corrosion potential ( $E_{corr}$ ), cathodic ( $b_c$ ) and anodic ( $b_a$ ) Tafel slopes, corrosion current density ( $I_{corr}$ ), coverage surface ( $\theta$ ) and inhibition efficiency (I%) are given in TABLE 3.

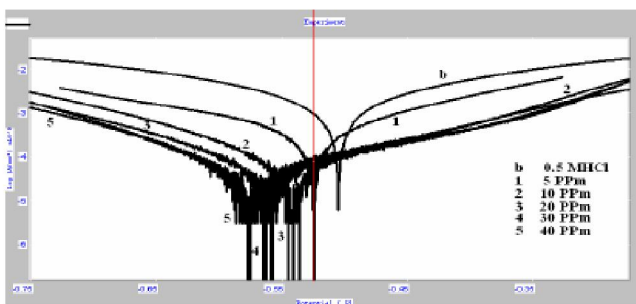


**Figure 10 : Polarization curves for carbon steel in M HCl in absence and presence of different concentrations of inhibitor**

**TABLE 3 : Parameters of potentiodynamic polarization of carbon steel electrode in 0.5M HCl containing various concentrations of the inhibitor (CVI) at 298±2K**

Conc. (PPm)	-E <sub>corr</sub> , mV	I <sub>corr</sub> , mA/cm <sup>2</sup>	R <sub>p</sub> , Ωcm <sup>2</sup>	b <sub>a</sub> , mV/dec	b <sub>c</sub> , mV/dec	C.R MMY	θ	E%
Blank	-526	0.42	76.36	168	-220	9.986	0.0	0.0
5	-542	0.12	90.19	154	-149	1.449	0.71	71.40
10	-548	0.09	523.46	155	-139	1.062	0.78	78.57
20	-560	0.08	-1683.02	204	-145	0.985	0.81	80.95
30	-577	0.07	185.39	174	-132	0.797	0.86	85.71
40	-573	0.04	-1599.64	174	-107	0.499	0.90	90.47

The data show that the I<sub>corr</sub> values decreased considerably with the increase in the inhibitor concentration. E<sub>corr</sub> shifted to more negative values, therefore these inhibitors acts predominantly as cathodic inhibitors<sup>[27]</sup> and consequently adsorption mechanism is much more likely at the cathodic sites. The effect of inhibitor type and concentration was observed on the values of b<sub>a</sub> and b<sub>c</sub>, so that these inhibitor obstruct the available surface area; it seems that film formed on the metallic surface became more uniform with concentration, while molecular structure may affect film resistance due to chemical bonding nature with metal-

lic surface. The inhibition efficiency, E (%), was calculated according to procedures developed by other authors<sup>[24]</sup>; it was obvious that the E (%) increases with increasing the inhibitor concentration. The inhibiting effect of these compounds was attributed to the formation of a chemical bonding between inhibitor and metallic surface<sup>[22-26]</sup>. Adsorption of compound through nitrogen element of primary amino group and oxygen molecules due to its capability of shearing lone pair electrons.

It is noteworthy that the results obtained from electrochemical measurements agree well with those obtained from both weight loss and open circuit potential determinations.

### EIS Measurements

Figure 11 Shows typical Nyquist impedance plots obtained for carbon steel electrode at an open circuit potential. The dotted curves represent the actual data and the solid line represents the best fit using the equivalent circuit shown in Figure 12 .The data obtained by fitting the equivalent circuit listed in TABLE 4 Indicate that the increase in inhibitor concentrations raises the polarization resistance (R<sub>p</sub>). It has been<sup>[12]</sup> reported that, the semicircles at high frequencies are generally associated with the relaxation of electrical double –layer capacitors, and the diameters of the high frequency capacitive loops can be considered as the charge – transfer resistance. This suggests that the electron transfer reaction corresponding to the second semicircle takes place through the surface layer, which limits mass transport (Warburg) or acts just like another resistor. The presence of the Warburg (W) impedance indicates that the mass transport is limited by the surface covered with organoamide inhibitor layers.

The inhibition efficiency, I%, of organoamide inhibitor for the carbon steel alloy electrode can then be calculated from the following equation:

$$I\% = \frac{R_p - R_s}{R_p} \times 100 \quad (9)$$

Where R<sub>s</sub> and R<sub>p</sub> are the charge transfer resistance in the blank and in the presence of organoamide inhibitor, respectively. A slight decrease of C<sub>dL</sub> values has been detected, which considers with the suggestion that organoamide inhibitor acts as corrosion inhibitor by adsorption onto the metallic surface<sup>[12,13]</sup>.

## Full Paper

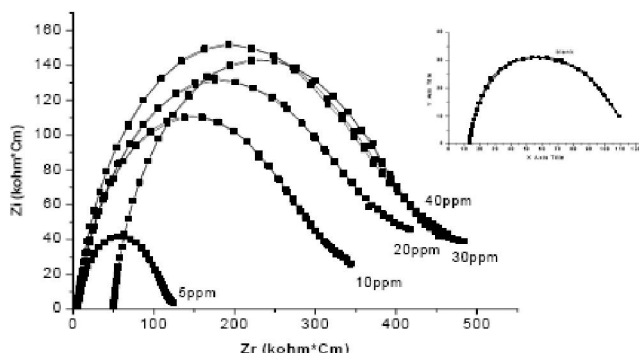


**Figure 11 :** Nyquist diagram for the carbon steel electrode immersed in 0.5 M HCl solution in absence and presence of different concentrations of inhibitor

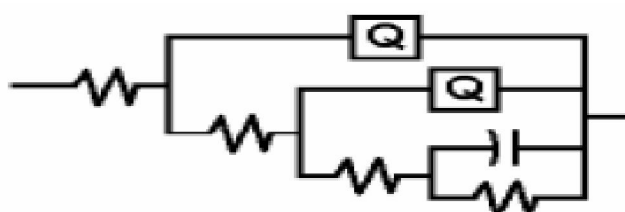


**Figure 12 :** Equivalent circuit  $R(Q(R(Q(R(CR))))$ ) used to fit experimental data represented in Figure 11

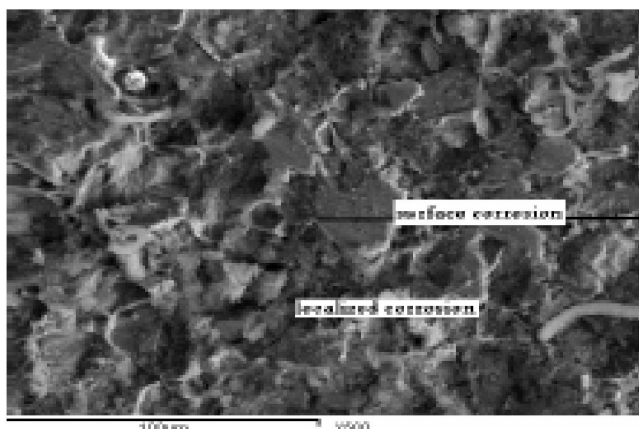


**Figure 13a**

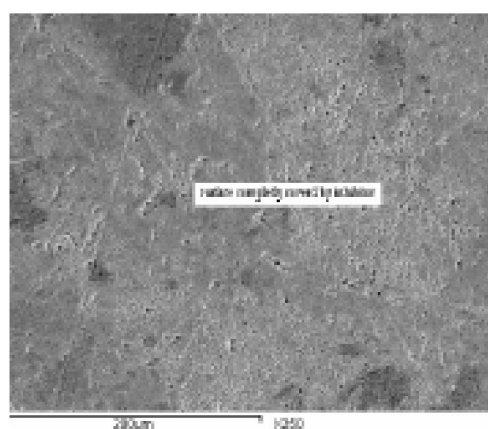


**Figure 13b**

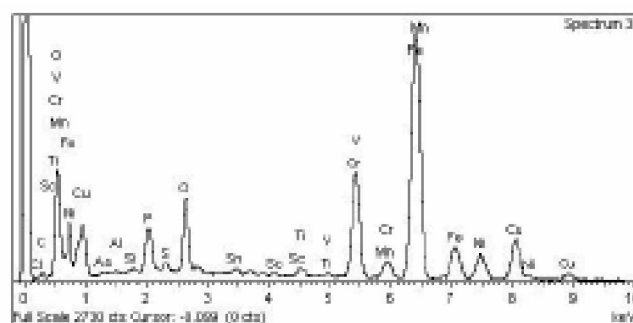


**Figure 13c**

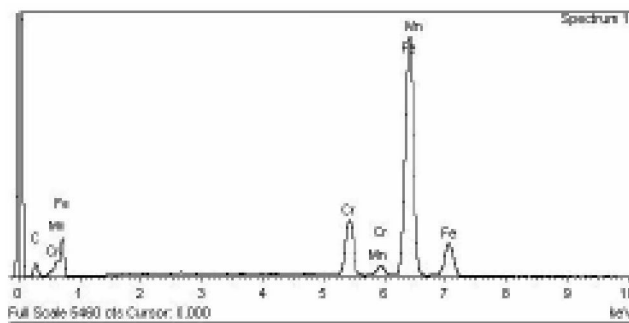


**Figure 13d**

**Figure 13 :** Scanning electron micrographs of carbon steel (a) sample after after immersion in 0.5M HCL solution without inhibitor X = 750, (b) sample X = 750 and sample after immersion in 0.5 M HCL solution containing 40 ppm of inhibitor and c, d the EDX

**TABLE 4 : Impedance measurements and inhibition efficiencies for carbon steel in 0.5M HCl containing different concentrations of inhibitor**

Conc. Ppm	$R_t$ $\Omega \text{cm}^2$	n	$C_{dl}$ $\mu\text{F cm}^{-2}$	I%
Blank	17.34	0.8764	9.88E-5	-
5	573.2	0.8934	1E-20	35
10	1E-7	0.9092	9.022E-6	61
20	67.64	0.8682	0.03438	73
30	1.197E-7	0.9178	5.556E-6	77
40	0.01399	0.8777	1.448E-5	81

### Scanning electron microscopy (SEM)

Scanning electron microscopy was used to examine the surface morphology of the carbon steel specimens immersed in 0.5M hydrochloric acid solution in absence and presence of 40 ppm of inhibitor. Figure 13a shows a characteristic of the immersion carbon steel, which is probably an oxide inclusion. On the other hand Figure 13b shows the surface of carbon steel specimen after immersion in 0.5M hydrochloric acid and 40ppm

**REFERENCES**

for 72 hr. Scanning electron micrographs reveal that the surface was strongly damaged by corrosion in absence of inhibitor however, much less damage of the surface is observed on the addition of the inhibitor to the acid solution proximally as a result of the formation of protective film of the inhibitor on the metal surface. The protective film formation of inhibitor on the surface of carbon steel in presence of 40 ppm of inhibitor. It appear as multilayer using magnification X= 750 and X= 2000, 750 and 2000 Figures 13c and d, respectively.

The results obtained from the (SEM) technique explain those obtained from weight loss method and all electro chemical data. Also, the EDX analysis Figures 13c and d shows the elemental analysis of the immersion of specimens in 0.5 M HCl without and with inhibitor, respectively.

**CONCLUSION**

- Synsization of the new corrosion inhibitor and characterization of it by FT.IR.
- Examination of the prepared compound as corrosion inhibitor at concentration 0.0, 5.0, 10.0. 20.0, 30.0 and 40.0 ppm.

Bentiss, M. Lagrene'e, Appl. Surf. Sci. 185 (2002) 197.

- The 0.5 M HCl used as electroyt solution.
- The evaluation carrid out by using weight loss, electropolarization, impedance, SEM and EDX techniques.
- The net results indicated the effect of inhibitor on the corrosion phenomena.

- [1] F.Bentiss, M.Lagrenée, M.Traisnel; Corrosion, **56**, 733 (**2000**).
- [2] V.S.Sastri; Corrosion Inhibitors Principles and Applications, John Wiley & Sons, New York, (**1998**).
- [3] I.L.Rosenfeld; Corrosion Inhibitors, McGraw-Hill, New York, (**1981**).
- [4] H.H.Uhlig, R.W.Rivie; Corrosion and Corrosion Control, John Wiley & Sons, NewYork, (**1985**).
- [5] L.F.Li, P.Caenen, J.P.; Corros. Sci., **50**, 804 (**2008**).
- [6] M.A.Quraishi, R.Sardar; Corrosion, **58**, 748 (**2002**).
- [7] M.Karakus, M.Sahin, S.Bilgic; Mater.Chem.Phys., **92**, 565 (**2005**).
- [8] E.M.Sherif, S.M.Park, Electrochim.Acta, **51**, 4665 (**2006**).
- [9] Qing Qua, Zhengzheng Hao, Lei Li, Wei Bai, Yongjun Liu, Zhongtao Ding; Corros.Sci, **51**, 569 (**2009**).
- [10] O.M.Abo-Elenien; Tikrit J.of Pure Sci., **11**(1), 201 (**2006**).
- [11] O.M.Abo-Elenien; J.Appl.Sci, **19**(11), 144 (**2004**).
- [12] O.M.Abo-Elenien; Mat.Sci.an Indian J., **2**(4-5), (**2006**).
- [13] O.M.Abo-Elenien, H.M.Abou-Alainin; Physical Chemistryan Indian J., **1**(4), (**2006**).
- [14] O.M.Abo-Elenien, H.M.Abu-Elainin; Egypt.J. Petrol., **1**, 9 (**2000**).
- [15] O.M.Abo-Elenien, H.M.Mohamed; Mans.Sci.Bull. (AChem.), **28**(1), (**2001**).
- [16] O.M.Abo-Elenien; Egypt.J.Appl.Sci., **19**(11), 161 (**2004**).
- [17] A.S.Fouda, Y.A.El-Ewady, O.M.Abo-Elenien, F.A.Agizah; Anti-Corrosion Methods and Materials, **55**(6), (**2008**).
- [18] O.M.Abo-Elenien; Chemistry: An Indian Journal, **1**(4), (**2006**).
- [19] M.A.Quraishi, F.A.Anvari; J.Appl.Electrochem., **36**, 309 (**2006**).
- [20] M.A.Quraishi, M.Z.A.Rafiquee, N.Saxena, S.Khan; J.Corros.Sci.Eng., **10**, (**2006**).
- [21] S.Sayed, E.R.Abd, H.Hamdi, A.Hassan, A.Mohammed; Mater.Chem.Phys., **78**, 337 (**2002**).
- [22] F.Bentiss, M.Traisnel, N.Chaibi, B.Mernari, H.Vezin, M.Lagrenée; Corr.Sci., **44**, 2271 (**2002**).
- [23] M.Lebrini, M.Lagrenée, H.Vezin, L.Gengembre, F.Bentiss; Corros.Sci., **47**, 485 (**2005**).
- [24] K.C.Emreg, M.Hayvalý; Mater.Chem.Phys., **83**, 209 (**2004**).
- [25] E.McCaerty; Corrosion Science, **47**, 3202 (**2005**).
- [26] F.Bentiss, M.Lebrini, M.Lagrene'e; Corrosion Science, **47**, 2915 (**2005**).
- [27] S.Zor, B.Yazyc, M.Erbil; Corrosion Science, **47**, 2700 (**2005**).